

A K-band phased array antenna system employing photonic true-time delay module

Yihong Chen, and Ray T. Chen

Microelectronics Research Center, The University of Texas at Austin

Austin, TX 78758

Email: yhchen@mail.utexas.edu

Abstract

A novel 1-to-64 (6-bit (2^6)) optical true-time delay module that can provide linear time delays ranging from 0 to 443.03 picoseconds is presented. The bandwidth of the fully packaged module is determined to be as high as 539 GHz. This true-time delay module is employed to control an eight-element K-band phased array antenna system. Far field patterns covering 18 GHz to 26.5 GHz are measured and compared with the simulated results to verify this module's wide instantaneous bandwidth. This module can be employed to control phased array antennas working at 5 GHz – 40 GHz.

Index Terms—Phased array antenna, true-time-delay, substrate guided wave, holographic optical element.

I. INTRODUCTION

Phased array antennas (PAAs) have the advantages of low visibility, high directivity and quick steering. Each antenna element of a phased array antenna must have the correct

phase condition to accomplish the desired beam scanning. However, the conventional electrical phase trimmer technique is an intrinsic narrow band technique that introduces beam squint. Recently, there has been growing interest in optical true-time-delay (TTD) modules. Optical TTD techniques are promising for squint-free beam steering of PAAs with features of wide bandwidth, compact size, reduced weights and low electromagnetic interference. Many kinds of optical TTD techniques have been proposed. These include the acoustic-optic technique [1], Fourier optics technique [2], [3], wavelength-multiplexing technique [4], [5], [6], [7], free space techniques [8], [9], [10], planar waveguide techniques [11], [12], fiber delay lines techniques [13], [14], [15], [16], and chirped fiber grating technique [17]. However, these modules are for applications with low RF frequencies, having higher insertion loss, limited resolution and complicated structures for steering control.

In a previous paper [18], a compact optical true-time-delay module based on substrate-guided wave structure was demonstrated. Delay intervals were obtained using holographic volume gratings that were recorded on a substrate. However, this module is restricted to PAAs working at low frequencies, since the delay interval is limited by the height of the substrate. Furthermore, large input coupling loss was introduced, which generated enormous insertion loss of the module.

We recently demonstrated an optical true-time-delay module for ultra wideband PAAs [19][20], having linear time delay steps ranging from 0 to 443.03 picoseconds. Moreover, the specially designed substrate is able to provide control signal for zero degree steering of PAAs that the structure in reference [18] unable to provide.

In this paper, a new TTD module is fabricated and packaged. The time delay error and bandwidth of the packaged device are specified. This module is employed to control an eight-element K-band PAA system. The wide instantaneous bandwidth of the TTD module is confirmed by measurements of far field patterns covering 18 GHz to 26.5 GHz.

II. STRUCTURE OF THE TTD MODULE

Fig. 1 illustrates the structure of the TTD module. This module is composed of eight sub-units. The optical signal, encoded by a microwave signal, is distributed among the eight sub-units using a 1-to-8 splitter. Each of the sub-units has a wedge of 21.5 degrees as indicated in Fig. 1. The wedges are coated with total reflect material to ensure that all the optical power is coupled into the substrate. The wedge angle introduces a bounce angle that is larger than the total internal reflection angle (41.8 degrees) at the interface of the substrate (BK-7 glass) and air. Adjacent to each wedge, the height of each sub-unit is maintained at the same value of t . The height of each sub-unit varies after one zig-zag bouncing and maintains at a fixed value for the rest of the sub-unit. Heights of the eight sub-units after the first zig-zag bouncing are from h_1 to h_8 , with a difference of Δh between adjacent sub-units. The difference Δh is pre-selected to satisfy the required delay combinations. The input signals from single-mode optical fibers are coupled into the module using graded index (GRIN) lenses. The substrate-guided wave zigzags within the substrate through total internal reflection. A portion of the substrate guided wave is extracted out each time the wave encounters the output holographic-grating coupler. The extracted optical waves are focused back into optical fibers using GRIN lenses. From Fig. 1, it can be seen that an eight by eight matrix of time delays is obtained. The position of

delay signals in the delay matrix is depicted by (i, j) , with i for the row number, j for the column number. Assuming the wedge angle is θ , the introduced time delay between signals at (i, j) and (k, l) is given by

$$\tau = \frac{2n}{c \cdot \cos(2\theta)} \cdot [(l-1) \cdot h_k - (j-1) \cdot h_i] \quad (1)$$

where c is the velocity of light in free space, n the refractive index of the substrate, h_i the height of the i th substrate, and h_k the height of the k th substrate.

Dupont photopolymer film HRF600*14-20 is used to form the holographic gratings. BK-7 glass is employed as the guided wave substrates. The surface dimension of each sub-unit is $90\text{mm} \times 11\text{mm}$. The step height t is equal to 2.6 mm. The height difference between the adjacent substrates is 0.147 mm. The heights after the first bouncing of the eight substrates are 3.600 mm, 3.747 mm, 3.894 mm, 4.041 mm, 4.188 mm, 4.335 mm, 4.482 mm, and 4.629 mm, respectively. Therefore, the volume of this module is $90\text{ mm} \times 88\text{ mm} \times 4.63\text{ mm}$. The eight by eight two-dimensional time delay matrix is shown in Table 1. The unit of time delays in Table 1 is picosecond. Time delays are calculated in reference to the first column of the delay matrix, providing linear time delays ranging from 0 to 443.03 picoseconds. If the distance interval of a PAA is equal to half of the working wavelength, these time delays can be employed to control PAAs working in the frequency range of 5 GHz – 40 GHz.

The K-band PAA used in the experiment has eight elements with a spacing interval of 0.3 inch between adjacent elements. By employing the true-time-delay settings for beam-squint-free phased array steering, we are able to calculate possible degrees of the steering of the K-band PAA to be $0, \pm 4.5^{\circ}, \pm 9.1^{\circ}, \pm 13.7^{\circ}, \pm 18.5^{\circ}, \pm 23.3^{\circ}, \pm 28.3^{\circ},$ and $\pm 33.6^{\circ}$,

as long as the columns of the matrix are used to provide delay steps as shown in Table 1. Even wider scanning range can be achieved with more sub-units or higher substrates.

III. CHARACTERISTICS OF THE TTD MODULE

The delay intervals are measured using a FPL-01T femtosecond Er-fiber laser from Calmar Optcom Inc., providing optical pulses around 0.2 picoseconds in the vicinity of 1550 nm. We measured the delay interval between the (1, 8) fan-out and the (8, 8) fan-out. As shown in Fig. 2, the measured delay interval is 98.49 ps, which is the same with the designed value.

Since the module may be used in field demonstration, the temperature effect on the module needs to be evaluated. The index of BK-7 glass has a temperature coefficient (dn/dt) of 5×10^{-6} . When the temperature varies from -25°C to 75°C ($\pm 50^{\circ}\text{C}$ deviation from room temperature), the index will have a change of ± 0.00025 . According to Eq. (1), the maximum change of time delay interval happens to the eighth column in Fig. 1, and the change is ± 0.0023 picoseconds. This change generates a maximum scanning shift of ± 1.2 seconds. This error is so small that it will not degrade the system performance seriously.

In order to determine the maximum frequency range of the microwave signals that can be carried by the TTD module, the bandwidth of the packaged device is specified. To evaluate the real bandwidth of this TTD module, a femtosecond laser and the Fourier spectrum analysis method are employed [21]. A FR-103MN autocorrelator from Femtochrome research Inc. is adopted to measure pulse widths before and after passing the fully packaged TTD module. Fourier transform of the two pulses generates bandwidth information of this TTD module, as shown in Fig. 3, indicating a 539GHz 3dB bandwidth.

IV. SYSTEM INTEGRATION AND MEASUREMENTS

The integrated K-band PAA system is demonstrated in Fig. 4. A microwave signal is generated by the heterodyne technique using two external cavity tunable semiconductor lasers. The optical carriers are evenly distributed among the eight sub-units of the TTD module by a 1-to-8 splitter. Desired time delays are added by this TTD module. In order to have a reference plane, a pre-adjustment delay bank is inserted at this point to compensate for the different delays caused by devices other than this TTD module. Afterwards, the microwave signals are detected by InGaAs high-speed photodetectors. The eight microwave signals with correct phase relationship are fed into eight antenna elements individually after amplification. The on/off states of photodetectors are controlled by a printed circuit board, which also serves as a microwave power uniformity controller. For single angle scanning of this K-band PAA, only one column of the fan-out beams from the TTD module is utilized. When the module is used as a beamforming network, all 64 fan-out beams from the TTD module are fed into 64 photodetectors, and all photodetectors are in the “on” states. Furthermore, microwave signals detected from the same row of the TTD module are first combined before they are fed to the PAA.

The optical heterodyne technique is employed to generate K-band microwave signals. Two external cavity tunable semiconductor lasers have the same center wavelength of 1550nm, same polarization, and a linewidth of 1MHz. Fig. 5 shows the experimental result of a 22 GHz RF signal generated by the heterodyne technique. The output power of tunable lasers are both -7dBm. The high-speed photodetector has a DC responsivity of 0.8A/W. The resulting RF signal power is -30.92dBm, 4dB less than the theoretical value.

Far field patterns of the K-band PAA are measured to verify the instantaneous microwave broad bandwidth. Various delay combinations are tested. Far field patterns are measured at three frequencies, the center frequency (22 GHz) and two edge frequencies (18 GHz, and 26.5 GHz). Fig. 6 compares the far field patterns at the three frequencies, with solid curves and curves with triangles denoting simulated results and measured results respectively. Note that in Fig.6, the fifth column of the TTD module shown in Fig.1 is employed to provide delay control signals for 18.5° scanning of the PAA. The locations of the main lobes covering all K band resulted from simulation and experiment agree very well. Furthermore, the PAA scanning angle is independent of microwave frequencies over the entire K-band, a primary feature of the true-time-delay approach.

In practice, information is transmitted in an encoded digital signal format. Therefore, a 2.5 Gbit/s random digital signal from Agilent 8133A pulse generator is employed to evaluate the degradation of the TTD link. The back-to-back Q factor of the 2.5 Gbit/s random digital signal is measured to be 50.42, while a Q factor of 10.20 is obtained after insertion of the TTD link with the eye diagram shown in Fig. 7. The main reasons for the degradation of Q factor and jitter are the noise coming from modulators, lasers, photodetectors and amplifiers. The Q factor does not change with scan angle due to the passive nature of the TTD module.

V. CONCLUSION

In conclusion, a novel 6-bit optical TTD module that can provide 0 to 443.03 picoseconds time delay has been fabricated, packaged and integrated into a K-band PAA system. This module is compact, easy to fabricate, and experimentally confirmed to provide

a wide instantaneous microwave bandwidth. Furthermore, this module can be employed to control phased array antennas working at 5 GHz – 40 GHz. In addition, this module can easily scale up for large arrays due to the miniaturization of the structure.

This research is currently supported by the AFOSR, BMDO, 3M Foundation, and the Advanced Technology Program of the State of Texas.

REFERENCES

- [1] L.H. Gesell, R.E. Feinleib, J.L. Lafuse, and T. M. Turpin, “Acousto-optic control of time delays for array beam steering,” *Optoelectronic Signal Processing for Phased-Array Antennas IV, Proc. SPIE*, vol. 2155, pp. 194-204, 1994.
- [2] Yoshihiko Konishi, etc., “Carrier-to-Noise Ratio and Sidelobe Level in a Two-Laser Mode Optically Controlled Array Antenna Using Fourier Optics”, *IEEE Trans. on Antennas and Propagation*, vol. 40, pp. 1459-1465, 1992.
- [3] G. A. Koepf, Optical processor for phased-array antenna beam formation, *Proc. SPIE*, vol. 477, pp. 75-81, 1984.
- [4] D.T.K. Tong and M.C. Wu, “A novel multiwavelength optically controlled phased array antenna with a programmable dispersion matrix,” *IEEE Photonics Technol. Lett.* Vol. 8, pp. 812-814, 1996.
- [5] R. Esman, M.Frankel, J. Dexter, L. Goldberg, M. Parent, D. Stiwell, and D. Cooper, “Fiber-optic prism true time-delay antenna feed,” *IEEE Photonics Technol. Lett.*, vol. 5, pp. 1347-1349, 1993.

- [6] A. Goutzoulis, D. Davies, and J. Zomp, "Hybrid electronic fiber optic wavelength-multiplexed system for true time-delay steering of phased array antennas," *Opt. Eng.*, vol. 31, pp. 2312-2322, 1992.
- [7] R. Soref, "Optical dispersion technique for time-delay beam steering," *Appl. Opt.*, vol. 31, pp. 7395-7397, 1992.
- [8] W. Ng, A. A. Walston, G. L. Taughlian, J. J. Lee, I. L. Newberg and N. Bernstein, "The first demonstration of an optically steered microwave phased array antenna using true-time-delay," *J. Lightwave Technol.*, vol. 9, pp. 1124-1131, 1991.
- [9] E. Ackerman, S. Wanuga, D. Kasemset, W. Minford, N. Thorsten, and J. Watson, "Integrated 6-bit photonic true-time-delay unit for lightweight 3-6GHz radar beamformer," *IEEE Trans. Microwave Theory Tech.*, vol. 6, pp. 681-684, 1992.
- [10] K. Kang, K. Deng, S. Koehler, I. Glesk, and P. Prucnal, "Fabrication of precision fiber-optic time delays with in situ monitoring for subpicosecond accuracy," *Appl. Opt.*, vol. 36, pp. 2533-2536, 1997.
- [11] R.Y.Loo, G.L.Tangonan, H.W. Yen, J.J.Lee, V.L.Jones, and J.Lewis, "5bit photonic time shifter for wideband arrays," *Electron. Lett.*, vol. 31, pp. 1521-1522, 1996.
- [12] H. R. Fetterman, Y. Chang, D. C. Scott, S. R. Forrest, F. M. Espiau, M. Wu, D. V. Plant, J. R. Kelly, A. Matteer, and W. H. Steier, "Optically controlled phased array radar receiver using SLM switched real time delays," *IEEE Microwave Guid. Wave Lett.*, vol. 5, pp. 414-416, 1995.
- [13] D. Dolfi, P. Joffre, J. Antoine, J. Huignard, D. Phillippet, and P. Granger, "Experimental demonstration of a phased-srray antenna optically controlled with phase and ime delays," *Appl. Opt.*, vol. 35, pp. 5293-5300, 1996.

- [14] I. Frigyes and A. Seeda, "Optically generated true-time delay in phased-array antennas," *IEEE Trans. Microwave Theory Tech.*, vol. 43, pp. 2378-2386, 1995.
- [15] Wenshen Wang, Yongqiang Shi, Weiping Lin, and James H. Bechtel, Waveguide Binary Photonic True-Time Delay Lines Using Polymer Integrated Switches and Waveguide Delays, *Proc. SPIE*, vol. 2844, pp. 200-211, 1996.
- [16] Kohji HORIKAWA, Ikuo OGAWA, Hiroyo OGAWA, and Tsutomu KITO, Photonic Switched True Time Delay Beam Forming Network Integrated on Silica Waveguide Circuits, *IEEE MTT-S Dig.*, TU1C-6, pp. 65-68, 1995.
- [17] Juan L. Corral, Javier Marti, "Optical Up-Conversion on Continuously Variable True-Time-Delay Lines Based on Chirped Gratings for Millimeter-Wave Optical Beamforming Networks", *IEEE Trans. On Microwave theory and techniques*, vol. 47, pp, 1315-1320, 1999.
- [18] Zhenhai Fu, Ray T. Chen, "Compact broadband 5-bit photonic true-time-delay module for phased-array antennas," *Optics Lett.*, vol. 23, pp. 522-524, 1998.
- [19] Yihong Chen, Ray T. Chen, "Photonic true time delay module for high frequency broad band phased array antenna," *Optoelectronic Interconnects and Packaging IV, Proc. SPIE*, vol. 4292, pp. 190-196, 2001.
- [20] Yihong Chen, Ray T. Chen, "A Fully Packaged True Time Delay Module for a K-band Phased Array Antenna System Demonstration," *IEEE Photonics Technol. Lett.*, August 2002
- [21] Z. Fu and R. Chen, "Five-bit substrate guided wave true-time delay module working at up to 2.4 THz with a packing density of 2.5 lines/cm² for phased array antenna applications," *Opt. Eng.*, vol. 37, pp. 1838-1844, 1998.

Figure captions

Table 1. The delay matrix and corresponding scanning angles of the TTD module

Fig. 1. Diagram of the structure of the 6-bit TTD module based on substrate-guided wave and holographic-grating couplers. GRIN, graded index.

Fig. 2. Measured delay interval between (1, 8) fan-out and (8, 8) fan-out.

Fig. 3. FFT power spectrum for the reference and dispersed pulses.

Fig. 4. Photograph of integrated K-band PAA system

Fig. 5. 22GHz RF signal generated by the optical heterodyne technique

Fig. 6. Comparison of far field patterns of the PAA at 18.5° scanning angle at three different frequencies: 18 GHz, 22 GHz, and 26.5 GHz.

Fig. 7. Eye diagram of a 2.5Gbit/s random digital signal after the optical TTD link measured by HP 83480A Digital Communications Analyzer

(a) back to back (b) after the optical TTD link

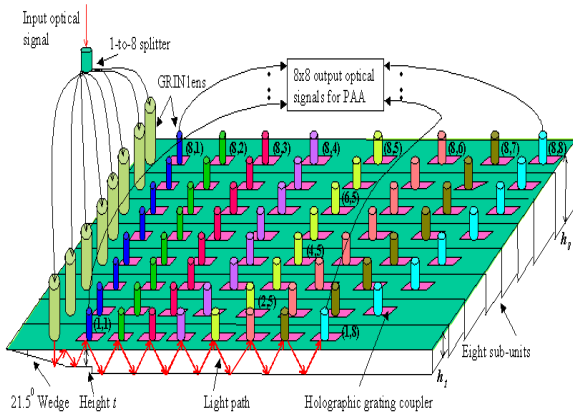


Fig. 1.

Column	1	2	3	4	5	6	7	8
Row								
1	0	49.22	98.44	147.66	196.88	246.10	295.32	344.54
2	0	51.23	102.46	153.69	204.92	256.15	307.38	358.61
3	0	53.24	106.48	159.72	212.96	266.20	319.44	372.68
4	0	55.25	110.50	165.75	221.00	276.25	331.50	386.75
5	0	57.26	114.52	171.78	229.04	286.30	343.56	400.82
6	0	59.27	118.54	177.81	237.08	296.35	355.62	414.89
7	0	61.28	122.56	183.84	245.12	306.40	367.68	428.96
8	0	63.29	126.58	189.87	253.16	316.45	379.74	443.03
Delay intervals	0	2.01	4.02	6.03	8.04	10.05	12.06	14.07
Scan angles	0°	±4.5°	±9.1°	±13.7°	±18.5°	±23.3°	±28.3°	±33.6°

Unit of time delay: Picosecond

Table 1.

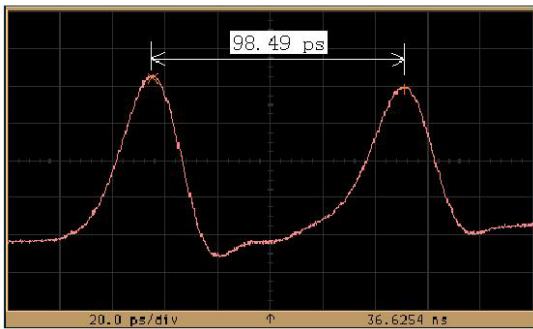


Fig. 2.

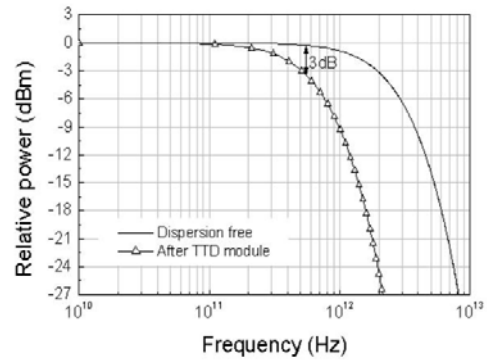


Fig. 3.

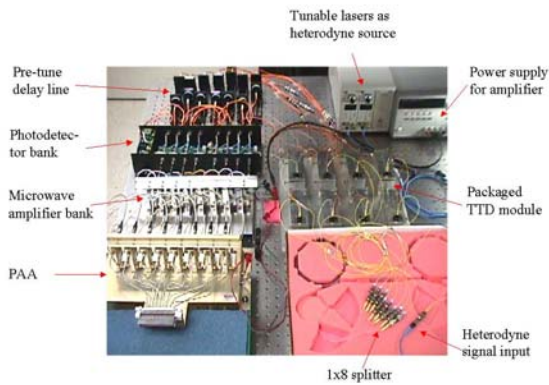


Fig. 4.

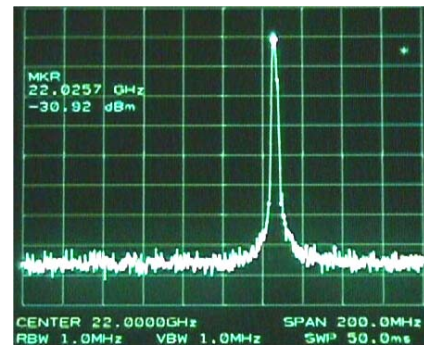


Fig. 5.

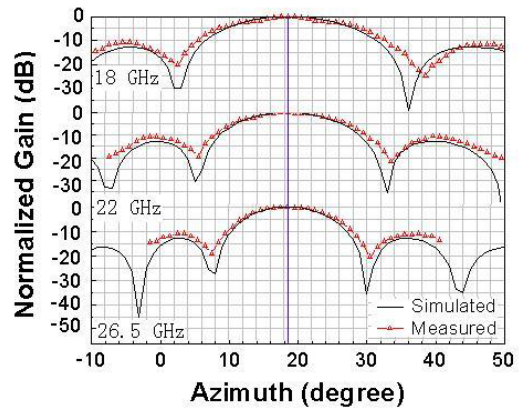


Fig. 6.

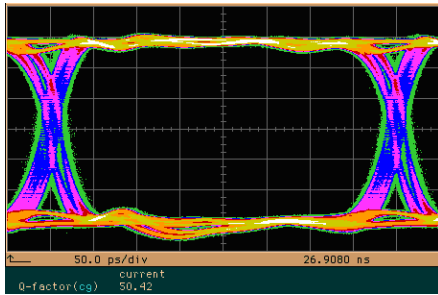


Fig. 7 (a)

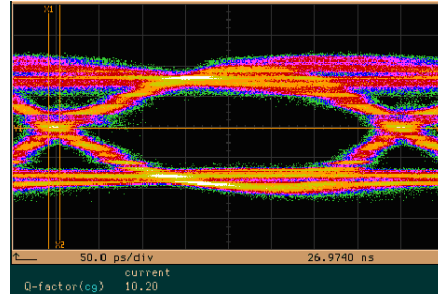


Fig. 7(b)